Some statistical properties of above-threshold excursions of random processes

2001 J. Phys. A: Math. Gen. 34 1231

(http://iopscience.iop.org/0305-4470/34/7/302)

INSTITUTE OF PHYSICS PUBLISHING JOURNAL OF PHYSICS A: MATHEMATICAL AND GENERAL

J. Phys. A: Math. Gen. **34** (2001) 1231–1246 www.iop.org/Journals/ja PII: S0305-4470(01)15391-6

Some statistical properties of above-threshold excursions of random processes

D Blacknell[1], **M Jahangir**[1], **F Piccolo**[1,2] **and R J A Tough**[3]

[1] DERA, St Andrew's Road, Malvern, Worcestershire WR14 3PS, UK
[2] Dipartimento di Ingegneria Elettronica, Via Claudio, 21, I-80125 Napoli, Italy
[3] T W Research, Harcourt Barn, Harcourt Road, Malvern, Worcestershire WR14 3DW, UK

E-mail: davebl@sar.dera.gov.uk, jahangir@sar.dera.gov.uk, piccolo@sar.dera.gov.uk and robert@twres1.freeserve.co.uk

Received 10 July 2000

Abstract

Correlated Gaussian random fields provide good models for a variety of physical phenomena including metallic and ocean surfaces, vegetation, geomorphology and turbulence. Their properties have been studied extensively yet some aspects of their behaviour are still not fully understood. In particular, the statistics of the number of samples within a correlated Gaussian random field which exceeds some threshold (i.e. the support of the random field) have not previously been analysed in depth. This threshold exceedence problem is discussed herein with closed-form expressions being presented for the variance of the support of the random field. Both one-dimensional (time series) and two-dimensional (image) cases are discussed and the results are extended to a correlated gamma-distributed random field which is appropriate for many non-Gaussian applications. The results are validated by comparison with numerical simulations and an assessment against approximate methods is made which reveals the superiority of the expressions presented. Potential applications of the theory are discussed with particular reference to the radar target detection problem and the modelling of breaking waves.

PACS number: 0250

1. Introduction

The Gaussian random process provides a useful and tractable model for many phenomena whose 'first-principles' description is precluded by its inherent complexity and a lack of detailed knowledge of its underlying mechanisms. The signals and noise encountered in communications and detection problems can be modelled by Gaussian processes evolving in time [1]; the spatial structures exhibited by Gaussian random fields enable them to capture the salient features of metallic and ocean surfaces, vegetation, geomorphology and turbulence [2]. Consequently, Gaussian processes have been studied intensively for many years. Nonetheless,

some of their properties are not yet fully understood; in particular, many of the characteristics of above-threshold excursions in Gaussian random processes have not been analysed in detail. This paper addresses one of the simplest of these problems: the statistics of the support of above-threshold excursions of time series and (two-dimensional) random fields. The expectation value of the duration or area of the support of such excursions is determined by the single-point statistics of the Gaussian process; its relation to the support of the entire random field is trivial. However, the calculation of the expectation value of the square of the excursions' support presents many more difficulties. In fact, Adler's text [2] states that no analytic progress can be made towards the solution of this problem beyond that made in the zero-threshold case, where the 'arcsine law' [3] reduces the problem to a relatively simple quadrature. In this paper we show how significant progress can, in fact, be made in the arbitrary threshold case. This analysis can be generalized in two ways: the characterization of the probability density function (PDF) of the excursion support and the extension of the analysis to non-Gaussian random processes which are important for radar and sonar image understanding [4]. Progress towards these goals has been limited but significant; an approximate analysis of the PDF is tractable in the large-threshold limit, while our exact results can be extended to the special, but practically important, non-Gaussian case provided by the gamma and χ^2 processes. Our results are then applied to time series and random fields of finite support; particular attention is paid to the variation in the mean-square excursion support as the support of the whole time series or field is progressively smaller than, comparable with and greater than that of the autocorrelation function of the Gaussian process. A selection of computer simulation results serves to both illustrate and verify our analysis.

2. Above-threshold excursions of a Gaussian random process

2.1. Derivation of fundamental results

The one- and two-point statistics of a Gaussian random process are particularly simple; consequently, we can set up and analyse formal expressions for the mean and mean-square values of the support of its above-threshold excursions. We will set these up in the case of a Gaussian random field u, whose values u vary with a two-dimensional spatial coordinate $\boldsymbol{r} \equiv (x, y)$; the corresponding, but simpler, results for a time series will then be written down by inspection. The autocorrelation of the values taken by u at two spatially separated points is given by

$$\langle u(\boldsymbol{r}_1)u(\boldsymbol{r}_2)\rangle = \left\langle u^2\right\rangle R(\boldsymbol{r}_1, \boldsymbol{r}_2) \tag{1}$$

without any real loss in generality we can take the mean and mean-square values of u to be zero and one, respectively. Thus we can write the probability density function of values of u as

$$P(u) = \frac{1}{\sqrt{2\pi}} \exp\left(-\frac{u^2}{2}\right) \tag{2}$$

while the joint PDF of the values u_1, u_2 taken at positions $\boldsymbol{r}_1, \boldsymbol{r}_2$ is

$$P(u_1, u_2) = \frac{1}{2\pi\sqrt{\left(1 - R(\boldsymbol{r}_1, \boldsymbol{r}_2)^2\right)}} \exp\left\{-\frac{\left(u_1^2 + u_2^2 - 2u_1u_2R(\boldsymbol{r}_1, \boldsymbol{r}_2)\right)}{2\left(1 - R(\boldsymbol{r}_1, \boldsymbol{r}_2)^2\right)}\right\}. \tag{3}$$

The number of excursions above a threshold U is given by

$$\sigma = \sum_{\boldsymbol{r}} I\left(u(\boldsymbol{r}) > U\right) \tag{4}$$

where $I(*)$ is the indicator function which takes the value 1 when the condition in the argument is satisfied and 0 otherwise. This is known as the support of the excursions. The mean value of the support of the excursions is thus given by

$$\langle \sigma \rangle = \sum_{\boldsymbol{r}} P(u(\boldsymbol{r}) > U) \tag{5}$$

which, in terms of a continuous spatial variable, becomes

$$\langle \sigma \rangle = \int_S \mathrm{d}^2 r \int_U^\infty \mathrm{d}u \; P(u) = \frac{A}{2} \operatorname{erfc}\left(\frac{U}{\sqrt{2}}\right). \tag{6}$$

Here A is the area of the support S of the whole random field and we have identified the complementary error function [5]; the corresponding result for a time series is obtained by replacing A by its duration T. The mean-square value of the support of above-threshold excursions is given by

$$\left\langle \sigma^2 \right\rangle = \sum_{\boldsymbol{r}_1} \sum_{\boldsymbol{r}_2} P(u(\boldsymbol{r}_1) > U, u(\boldsymbol{r}_2) > U) \tag{7}$$

which in terms of a continuous spatial variable, becomes

$$\begin{aligned}\left\langle \sigma^2 \right\rangle &= \int_S \mathrm{d}^2 r_1 \int_S \mathrm{d}^2 r_2 \int_U^\infty \mathrm{d}u_1 \int_U^\infty \mathrm{d}u_2 \; P(u_1, u_2) \\ &= \int_S \mathrm{d}^2 r_1 \int_S \mathrm{d}^2 r_2 \int_U^\infty \mathrm{d}u_1 \\ &\quad \times \int_U^\infty \mathrm{d}u_2 \, \frac{1}{2\pi\sqrt{\left(1 - R(\boldsymbol{r}_1, \boldsymbol{r}_2)^2\right)}} \exp\left\{ -\frac{u_1^2 + u_2^2 - 2u_1 u_2 R(\boldsymbol{r}_1, \boldsymbol{r}_2)}{2\left(1 - R(\boldsymbol{r}_1, \boldsymbol{r}_2)^2\right)} \right\}. \end{aligned} \tag{8}$$

In the time series case we have

$$\begin{aligned}\left\langle \sigma^2 \right\rangle &= \int_0^T \mathrm{d}t_1 \int_0^T \mathrm{d}t_2 \int_U^\infty \mathrm{d}u_1 \int_U^\infty \mathrm{d}u_2 \; P(u_1, u_2) \\ &= \int_0^T \mathrm{d}t_1 \int_0^T \mathrm{d}t_2 \int_U^\infty \mathrm{d}u_1 \\ &\quad \times \int_U^\infty \mathrm{d}u_2 \, \frac{1}{2\pi\sqrt{\left(1 - R(t_1, t_2)^2\right)}} \exp\left\{ -\frac{u_1^2 + u_2^2 - 2u_1 u_2 R(t_1, t_2)}{2\left(1 - R(t_1, t_2)^2\right)} \right\}. \end{aligned} \tag{9}$$

Thus we see that $\langle \sigma \rangle$ is independent of the correlation function R. However, $\left\langle \sigma^2 \right\rangle$ does depend on R and its spatial variation within S; expression (8) has been derived elsewhere [2, 6]. When the threshold U takes the value zero the integrals over u_1, u_2 can be carried out analytically to give

$$\left\langle \sigma^2 \right\rangle_{U=0} = \frac{A^2}{4} + \frac{1}{2\pi} \int_S \mathrm{d}^2 r_1 \int_S \mathrm{d}^2 r_2 \sin^{-1}\left(R(\boldsymbol{r}_1, \boldsymbol{r}_2)\right). \tag{10}$$

However, the apparent intractability of the integral over u_1, u_2 has presented a barrier to further progress in the general case. This can be overcome by first writing the joint probability of the correlated Gaussian variables in terms of the characteristic function

$$P(u_1, u_2) = \frac{1}{(2\pi)^2} \int_{-\infty}^\infty \mathrm{d}k_1 \int_{-\infty}^\infty \mathrm{d}k_2 \; \exp\left\{-\mathrm{i}(k_1 u_1 + k_2 u_2)\right\} \exp\left\{-\tfrac{1}{2}\left(k_1^2 + k_2^2 + 2k_1 k_2 R\right)\right\}. \tag{11}$$

Since

$$\int_U^\infty \mathrm{d}u_1 \exp\left(-\mathrm{i}k_1 u_1\right) = \frac{\exp\left(-\mathrm{i}k_1 U\right)}{\mathrm{i}k_1} \tag{12}$$

we see that

$$\begin{aligned}\hat{\sigma}(R)^2 &\equiv \int_U^\infty \mathrm{d}u_1 \int_U^\infty \mathrm{d}u_2\, P(u_1, u_2) \\ &= -\frac{1}{(2\pi)^2}\int_{-\infty}^\infty \mathrm{d}k_1 \int_{-\infty}^\infty \mathrm{d}k_2\, \frac{\exp(-\mathrm{i}(k_1+k_2)U)}{k_1 k_2} \exp\left\{-\tfrac{1}{2}\left(k_1^2 + k_2^2 + 2k_1k_2R\right)\right\}\end{aligned} \tag{13}$$

so that

$$\frac{\mathrm{d}\hat{\sigma}(R)^2}{\mathrm{d}R} = -\frac{1}{(2\pi)^2}\int_{-\infty}^\infty \mathrm{d}k_1 \int_{-\infty}^\infty \mathrm{d}k_2 \exp\left\{-\mathrm{i}(k_1+k_2)U\right\} \exp\left\{-\tfrac{1}{2}\left(k_1^2 + k_2^2 + 2k_1k_2R\right)\right\}. \tag{14}$$

Comparison with equation (11) reveals that

$$\frac{\mathrm{d}\hat{\sigma}(R)^2}{\mathrm{d}R} = P(U,U) = \frac{1}{2\pi\sqrt{1-R^2}} \exp\left\{-\frac{U^2}{(1+R)}\right\} \tag{15}$$

and this simple differential equation may be solved to give

$$\hat{\sigma}(R)^2 = \hat{\sigma}(R_0)^2 + \frac{1}{2\pi}\int_{R_0}^R \mathrm{d}\eta\, \frac{1}{\sqrt{1-\eta^2}} \exp\left\{-\frac{U^2}{(1+\eta)}\right\}. \tag{16}$$

If $R_0 = 0$ then the bivariate Gaussian is uncorrelated so that

$$\hat{\sigma}(0)^2 = \frac{1}{2\pi}\left\{\int_U^\infty \mathrm{d}u \exp\left(-\frac{u^2}{2}\right)\right\}^2 = \left\{\frac{1}{2}\operatorname{erfc}\left(\frac{U}{\sqrt{2}}\right)\right\}^2. \tag{17}$$

Alternatively, if $R_0 = 1$ then the bivariate Gaussian is fully correlated and the joint PDF is proportional to $\delta(x-y)$ so that

$$\hat{\sigma}(1)^2 = \frac{1}{\sqrt{2\pi}}\int_U^\infty \mathrm{d}u \exp\left(-\frac{u^2}{2}\right) = \frac{1}{2}\operatorname{erfc}\left(\frac{U}{\sqrt{2}}\right) \tag{18}$$

whilst if $R_0 = -1$ then the bivariate Gaussian is fully anticorrelated and the joint PDF is proportional to $\delta(x+y)$ so that, if $U \geqslant 0$,

$$\hat{\sigma}(-1)^2 = 0. \tag{19}$$

In this latter case, substitution into equation (16) gives the simple result for $U \geqslant 0$ that

$$\hat{\sigma}(R)^2 = \frac{1}{2\pi}\int_{-1}^{R(r_1,r_2)} \mathrm{d}\eta\, \frac{1}{\sqrt{1-\eta^2}} \exp\left\{-\frac{U^2}{(1+\eta)}\right\}. \tag{20}$$

In some ways equation (20) is our principal result; the remainder of the paper will be concerned with its analysis, application and generalization.

2.2. Asymptotic limits

2.2.1. Small-threshold limit. When the threshold u is set to zero (20) leads to the familiar result (10). However, when the threshold u is small but not zero we consider the integral

$$F(R) = \int_0^R \mathrm{d}\eta \, \frac{1}{\sqrt{1-\eta^2}} \exp\left\{-\frac{U^2}{1+\eta}\right\}. \tag{21}$$

Expansion of the exponential term in the integrand leads to

$$F(R) = \sin^{-1}(R) + \sum_{n=1}^{\infty} \frac{(-U^2)^n}{n!} \int_0^R \frac{\mathrm{d}\eta}{(1-\eta^2)^{1/2}(1+\eta)^{n+1/2}}. \tag{22}$$

The integrals occurring in this series are best evaluated by recursion. If we define

$$P_n = \int_0^R \frac{\mathrm{d}\eta}{(1-\eta^2)^{1/2}(1+\eta)^n} \tag{23}$$

then

$$P_n(R) = P_{n-1}(R) - \int_0^R \frac{\eta \, \mathrm{d}\eta}{(1-\eta^2)^{1/2}(1+\eta)^n} \tag{24}$$

which an integration by parts reduces to

$$P_n(R) = \left(\frac{n-1}{2n-1}\right) P_{n-1}(R) + \frac{1}{(2n-1)} \left(1 - \frac{(1-R^2)^{1/2}}{(1+R)^n}\right). \tag{25}$$

From this we see straightaway that

$$P_1(R) = 1 - \frac{(1-R^2)^{1/2}}{(1+R)} \tag{26}$$

from which the other integrals can be generated, if required. Here we merely note that

$$F(R) = \sin^{-1}(R) - \left(1 - \frac{(1-R^2)^{1/2}}{(1+R)}\right) U^2 + \mathrm{O}(U^4). \tag{27}$$

2.2.2. Large-threshold limit. To determine the large-threshold behaviour of (20) we need to transform the integrand such that it contains a term of the form $\exp(-sU^2)$ and also transform the integration limits to cover the range $[0, \infty)$ so that an asymptotic expansion can be obtained by using Watson's lemma [7]. This is achieved by making the substitution

$$s = \frac{1}{(1+\eta)} - \frac{1}{(1+R)} \tag{28}$$

which results in a new integral formulation

$$\hat{\sigma}(R)^2 = \frac{1}{2\pi} \exp\left\{-\frac{U^2}{(1+R)}\right\} \frac{(1+R)^{3/2}}{(1-R)^{1/2}} \times \int_0^{\infty} \mathrm{d}s \, \frac{\exp(-sU^2)}{(1+(1+R)s)\sqrt{(1+2(1+R)s/(1-R))}}. \tag{29}$$

Use of Watson's lemma then gives

$$\hat{\sigma}(R)^2 \sim \frac{1}{2\pi U^2} \exp\left\{-\frac{U^2}{(1+R)}\right\} \frac{(1+R)^{3/2}}{(1-R)^{1/2}} \left[1 - \frac{(1+R)(2-R)}{(1-R)U^2} + \mathrm{O}(U^{-4})\right]. \tag{30}$$

2.3. Probability density function

So far we have considered only exact expressions for the mean and mean-square values of the support of above-threshold excursions. These provide us with only limited insight into the form of the PDF of the above-threshold support. However, it is possible to construct such a PDF in the limit of a large threshold. To this end we note (see Adler [2, chapter 6]) the following properties of high-threshold excursions in a random field with a support of area A.

(a) The mean number of excursions above a threshold U is given by

$$\langle N\rangle = A\sqrt{\frac{|\det\Lambda|}{(2\pi)^3}}U\exp\left(-\frac{U^2}{2}\right) \tag{31}$$

where

$$\Lambda = \begin{pmatrix} R_{xx} & R_{xy} \\ R_{yx} & R_{yy} \end{pmatrix}$$

is a matrix of derivatives of the normalized correlation function of the random variable u. This has been simplified by exploiting the assumed translational invariance of the system; $R_{xx} \equiv \partial^2 R/\partial x_1 \partial x_2|_{r_1=r_2}$, etc

(b) The number n of excursions in the area A is Poisson distributed, i.e.

$$P(n) = \frac{\langle N\rangle^n}{n!}\exp(-\langle N\rangle). \tag{32}$$

(c) The support s of an individual excursion above the threshold has a negative exponential distribution:

$$\begin{aligned} P(s) &= \gamma U^2 \exp\left(-\gamma U^2 s\right) \\ \gamma &= \frac{1}{2\pi}\sqrt{|\det\Lambda|}. \end{aligned} \tag{33}$$

Thus if there are n excursions above the threshold in the area A, the PDF of their total support is given by

$$P(\sigma, n) = \frac{(\gamma U^2)^n \sigma^{n-1}}{(n-1)!}\exp\left(-\gamma U^2\sigma\right). \tag{34}$$

As n is a Poisson-distributed random variable we can form the PDF of the total area of above-threshold excursions as

$$\begin{aligned} P(\sigma) &= \sum_n P(\sigma, n)P(n) \\ &= 2\exp\left(-\langle N\rangle\right)\delta(\sigma) + \exp\left(-\langle N\rangle - \gamma U^2\sigma\right)\langle N\rangle\gamma U^2 \sum_{n=0}^{\infty}\frac{\langle N\rangle^n}{n!}\frac{\left(\gamma U^2\right)^n\sigma^n}{(n+1)!} \\ &= 2\exp\left(-\langle N\rangle\right)\delta(\sigma) + \exp\left(-\langle N\rangle - \gamma U^2\sigma\right)\langle N\rangle\sqrt{\frac{\langle N\rangle\gamma U^2}{\sigma}}I_1\left(2\sqrt{\langle N\rangle\gamma U^2\sigma}\right). \end{aligned} \tag{35}$$

For $n = 0$, $P(\sigma, n)$ has been identified with the delta function. Furthermore, the infinite series occurring here has been related to the expansion of the modified Bessel function of the first kind and first order [5, equation (9.6.10)].

PDFs of this form have been considered in a variety of contexts. The work of Clements and Yurtsever on the breaking area model of sea clutter [8] is one of these, two others are provided by Cox and Miller [9]. Thus exercise 5 in chapter 4 of this text presents (35) as the PDF of a sum of a Poisson-distributed number of independent exponentially distributed random variables, while exercise 9 in chapter 5 highlights an interesting connection with the diffusive description of the branching process. Once we have constructed this PDF we can calculate its moments. In particular, the mean and mean square of σ can be evaluated to give

$$\begin{aligned} \langle\sigma\rangle &= \frac{\langle N\rangle}{\gamma U^2} = \frac{A}{\sqrt{2\pi}U}\exp\left(-\frac{U^2}{2}\right) \\ \left\langle\sigma^2\right\rangle &= \frac{\langle N\rangle}{\left(\lambda U^2\right)^2}\left(2+\langle N\rangle\right) \\ \frac{\mathrm{var}(\sigma)}{\langle\sigma\rangle^2} &= \frac{2}{\langle N\rangle}. \end{aligned} \tag{36}$$

The first of these is the high-threshold asymptotic form of (4).

3. Above-threshold excursions of gamma and χ squared random processes

The mean-square value of the support of above-threshold excursions of a correlated Gaussian process has been analysed using an approach based on the characteristic function; it will now be seen how a similar approach can be applied to a class of correlated gamma processes. This is of importance for applications such as detection in radar and sonar images where the background clutter is better modelled by non-Gaussian distributions such as the gamma distribution [4].

The general form of the multivariate Gaussian PDF, of which [3] is the bivariate case, arises from the superposition of a number of uncorrelated Gaussian contributions reflecting an underlying physical mechanism. This multivariate Gaussian PDF satisfies the necessary conditions that the marginal distributions are Gaussian and that the covariance matrix has the desired form. It is possible to construct other joint PDFs which satisfy the same conditions but these do not have the same physical basis and are thus of limited physical importance. In contrast, as has been observed by Blacknell [10], there are no such compelling arguments which might identify the joint PDF of a correlated random variable with gamma-distributed marginals. There is, however, a class of correlated gamma processes which is analytically tractable and for which the evaluation of the mean-square value of the support of above-threshold excursions can be carried through much as in the Gaussian case.

Consider two correlated, positive-valued random variables z_1, z_2 for which the characteristic function is given by

$$C(s_1, s_2) = \frac{1}{\left(1+\alpha(s_1+s_2)+\alpha^2(1-\zeta)s_1s_2\right)^{\nu}}. \tag{37}$$

It is straightforward to show, using Laplace inversion techniques, that the marginal PDFs of z_1, z_2 each have the familiar gamma form

$$P(z) = \frac{1}{\alpha^{\nu}\Gamma(\nu)}z^{\nu-1}\exp\left(-\frac{z}{\alpha}\right) \tag{38}$$

where ν is the order parameter and $\alpha = \mu/\nu$ gives a mean μ and variance μ^2/ν. The characteristic function may be used to determine the moment $\langle z_1 z_2 \rangle$ by taking the derivative with respect to s_1, s_2 and setting $s_1 = 0$, $s_2 = 0$ to give

$$\langle z_1 z_2 \rangle = \frac{\mu^2}{\nu}(\nu + \zeta) \tag{39}$$

which, when normalized, gives the correlation coefficient ζ. On taking the Laplace transform of (37), the full bivariate PDF is found to be

$$\begin{aligned} P(z_1, z_2) &= \frac{1}{(2\pi \mathrm{i})^2} \int_{C_1} \mathrm{d}s_1 \int_{C_2} \mathrm{d}s_2 \, \frac{\exp(s_1 z_1 + s_2 z_2)}{\left(1 + \alpha(s_1 + s_2) + \alpha^2(1-\zeta)s_1 s_2\right)^{\nu}} \\ &= \frac{(z_1 z_2)^{(\nu-1)/2}}{\alpha^{\nu+1}(1-\zeta)\zeta^{(\nu-1)/2}\Gamma(\nu)} \exp\left(-\frac{(z_1+z_2)}{\alpha(1-\zeta)}\right) I_{\nu-1}\left(\frac{2\sqrt{\zeta z_1 z_2}}{\alpha(1-\zeta)}\right). \end{aligned} \tag{40}$$

This PDF describes the two correlated χ^2 variables which result when a number of correlated Gaussian pairs are squared and added together (Armstrong and Griffiths [11]). Wong [12] obtains an expression closely related to (40) by explicit solution of the Fokker–Planck equation satisfied by the conditional probability $P(z_2|z_1)$ for values z_1, z_2 of a gamma-Markov process occurring at a time t apart. The expressions are identical when the identification $\zeta = \exp(-t)$ is made.

The mean value of the support of the excursions is given by

$$\langle \sigma \rangle = \int_S \mathrm{d}^2 r \int_U^{\infty} \mathrm{d}u \, P(z) = A \frac{\Gamma(\nu, U/\alpha)}{\Gamma(\nu)} \tag{41}$$

whilst the mean-square value is obtained from $\hat{\sigma}(\zeta)^2$. Following the same reasoning as in the previous section gives

$$\begin{aligned} \hat{\sigma}(\zeta)^2 &= \int_U^{\infty} \mathrm{d}z_1 \int_U^{\infty} \mathrm{d}z_2 \, P(z_1, z_2) \\ &= \frac{1}{(2\pi \mathrm{i})^2} \int_{C_1} \mathrm{d}s_1 \int_{C2} \mathrm{d}s_2 \, \frac{1}{s_1 s_2} \frac{\exp(s_1 U + s_2 U)}{\left(1 + \alpha(s_1 + s_2) + \alpha^2(1-\zeta)s_1 s_2\right)^{\nu}} \end{aligned} \tag{42}$$

so that

$$\begin{aligned} \frac{\mathrm{d}\hat{\sigma}(\zeta)^2}{\mathrm{d}\zeta} &= \frac{\alpha^2 \nu}{(2\pi \mathrm{i})^2} \int_{C_1} \mathrm{d}s_1 \int_{C_2} \mathrm{d}s_2 \frac{\exp(s_1 U + s_2 U)}{\left(1 + \alpha(s_1 + s_2) + \alpha^2(1-\zeta)s_1 s_2\right)^{\nu+1}} \\ &= \frac{1}{(1-\zeta)\zeta^{\nu/2}\Gamma(\nu)} \left(\frac{U}{\alpha}\right)^{\nu} \exp\left(-\frac{2U}{\alpha(1-\zeta)}\right) I_{\nu}\left(\frac{2U\sqrt{\zeta}}{\alpha(1-\zeta)}\right). \end{aligned} \tag{43}$$

Taking the fully decorrelated limit as an initial value, integration of this differential equation gives

$$\hat{\sigma}(\zeta)^2 = \left(\frac{\Gamma(\nu, U/\alpha)}{\Gamma(\nu)}\right)^2 + \frac{1}{\Gamma(\nu)} \left(\frac{U}{\alpha}\right)^{\nu} \int_0^{\zeta} \frac{\mathrm{d}\xi}{(1-\xi)\xi^{\nu/2}} \exp\left(-\frac{2U}{\alpha(1-\xi)}\right) I_{\nu}\left(\frac{2U\sqrt{\xi}}{\alpha(1-\xi)}\right) \tag{44}$$

where use has been made of the incomplete gamma function $\Gamma(\nu, \varphi) = \int_{\varphi}^{\infty} \mathrm{d}t \, t^{\nu-1} \exp(-t)$.

4. The evaluation of $\langle\sigma\rangle$ and $\langle\sigma^2\rangle$ for stationary Gaussian processes

The mean value of the support of above-threshold excursions of a Gaussian process is given by the relatively simple result (6) whilst, on substituting the result (20) into (8), an expression for the mean-square value of the above-threshold support is obtained. In principle, this expression can be evaluated numerically although, in practice, this will involve an integration over five variables for the two-dimensional case which makes the calculation very computationally demanding. However, in the commonly occurring case where the Gaussian process is stationary, i.e. the correlation function satisfies the condition $R(\boldsymbol{r}_1, \boldsymbol{r}_2) = R(\boldsymbol{r}_1 - \boldsymbol{r}_2)$, it is possible to replace the integrations over the separate coordinates $\boldsymbol{r}_1, \boldsymbol{r}_2$ by an integration over the single difference coordinate $\boldsymbol{r}_1 - \boldsymbol{r}_2$. The integration over the dummy variable η in (20) can also be eliminated by an integration by parts. By using these simplifications it is possible to calculate $\langle\sigma\rangle^2$ rapidly and accurately for Gaussian random fields with arbitrary correlation properties.

Consider first the one-dimensional time-series case. Using a number of integrations by parts, the following identity may be obtained:

$$\int_0^T \mathrm{d}t_1 \int_0^T \mathrm{d}t_2\, \phi(t_1 - t_2) = \int_0^T \mathrm{d}t\, (T - t)\hat{\phi}(t) \tag{45}$$

where $\hat{\phi}(t) = \phi(t) + \phi(-t)$. To make contact with the calculation of $\langle\sigma^2\rangle$, the function $\phi(t)$ is identified with the function $\hat{\sigma}(R(t))^2$. The first term on the right-hand side of (45) can be written as

$$\begin{aligned}\int_0^T \mathrm{d}t\, T\hat{\phi}(t) &= T\int_{-T}^{T} \mathrm{d}t\, \phi(t) \approx T\int_{-\infty}^{\infty} \mathrm{d}t\, \phi(t) \\ &= \frac{T}{2\pi}\int_{-\infty}^{\infty}\mathrm{d}t \int_{-1}^{R(t)} \mathrm{d}\eta\, \frac{1}{\sqrt{1-\eta^2}} \exp\left(-\frac{U^2}{(1+\eta)}\right)\end{aligned} \tag{46}$$

which dominates as the area of the support of the function becomes larger; the other terms are the lower-order corrections. Thus (46) provides an approximation which reduces the number of integrations required in a numerical calculation from three to two. However, alternatively, a further integration by parts of (45) yields

$$\begin{aligned}\int_0^T \mathrm{d}t_1 \int_0^T \mathrm{d}t_2\, \phi(t_1 - t_2) &= \frac{T^2}{2}\hat{\phi}(T) - \frac{1}{2}\int_0^T \mathrm{d}t\, \frac{\mathrm{d}\hat{\phi}(t)}{\mathrm{d}t}(2Tt - t^2) \\ &= \frac{1}{2\pi}\left\{T^2 \int_0^{R(t)} \mathrm{d}\eta\, \frac{1}{\sqrt{1-\eta^2}} \exp\left(-\frac{U^2}{(1+\eta)}\right)\right. \\ &\quad \left. - \int_0^T \mathrm{d}t\, \frac{1}{\sqrt{1-R(t)^2}} \exp\left(-\frac{U^2}{(1+R(t))}\right)\frac{\mathrm{d}R(t)}{\mathrm{d}t}(2Tt - t^2)\right\}\end{aligned} \tag{47}$$

where time-reversal invariance of the autocorrelation function, $R(t) = R(-t)$, has been exploited. The expression (47) provides an exact method for calculating $\langle\sigma^2\rangle$ which requires only a single integration, thus making it amenable to numerical calculation.

The case of a two-dimensional image follows similar reasoning. Several integrations by parts yield the identity

$$\begin{aligned}&\int_0^L \mathrm{d}x_1 \int_0^L \mathrm{d}y_1 \int_0^L \mathrm{d}x_2 \int_0^L \mathrm{d}y_2\, \Phi(x_1 - x_2, y_1 - y_2) \\ &\qquad = \int_0^L \mathrm{d}x \int_0^L \mathrm{d}y\, (L - x)(L - y)\hat{\Phi}(x, y)\end{aligned} \tag{48}$$

where $\hat{\Phi}(x, y) = \Phi(x, y) + \Phi(x, -y) + \Phi(-x, y) + \Phi(-x, -y)$. The first term on the right-hand side of (48) can be written as

$$\int_0^L \mathrm{d}x \int_0^L \mathrm{d}y\, L^2 \hat{\Phi}(x, y) = L^2 \int_{-L}^L \mathrm{d}x \int_{-L}^L \mathrm{d}y\, \Phi(x, y) \approx L^2 \int_{-\infty}^{\infty} \mathrm{d}x \int_{-\infty}^{\infty} \mathrm{d}y\, \Phi(x, y)$$
$$= \frac{L^2}{2\pi} \int_{-\infty}^{\infty} \mathrm{d}x \int_{-\infty}^{\infty} \mathrm{d}y \int_{-1}^{R(x,y)} \mathrm{d}\eta\, \frac{1}{\sqrt{1-\eta^2}} \exp\left(-\frac{U^2}{(1+\eta)}\right) \tag{49}$$

thus providing an approximation which reduces the number of integrations required from five to three. An alternative approach is based on the observation that

$$(L - x)(L - y) = \tfrac{1}{2}\nabla \cdot \left(\boldsymbol{r}\left(L^2 - \tfrac{2}{3}L(x + y) + \tfrac{1}{2}xy\right)\right) \tag{50}$$

so that

$$\int_0^L \mathrm{d}x \int_0^L \mathrm{d}y\, (L - x)(L - y)\hat{\Phi}(x, y)$$
$$= -\tfrac{1}{2} \int_0^L \mathrm{d}x \int_0^L \mathrm{d}y \left(L^2 - \tfrac{2}{3}L(x + y) + \tfrac{1}{2}xy\right) \boldsymbol{r} \cdot \nabla\hat{\Phi}(x, y)$$
$$+\tfrac{1}{2} \oint \mathrm{d}\boldsymbol{l} \cdot \boldsymbol{r} \left(L^2 - \tfrac{2}{3}L(x + y) + \tfrac{1}{2}xy\right)\hat{\Phi}(x, y). \tag{51}$$

The line integral is taken round a square circuit with corners at $(0, 0)$, $(0, L)$, (L, L), $(L, 0)$. If the sides, going around anticlockwise from $(0, 0)$, are labelled (a), (b), (c), (d), respectively, then on sides (a) and (d) $\mathrm{d}\boldsymbol{l} \cdot \boldsymbol{r} = 0$, whilst on (b) and (c) $\mathrm{d}\boldsymbol{l} \cdot \boldsymbol{r} = L\,\mathrm{d}y$ and $L\,\mathrm{d}x$, respectively. Thus (51) can be simplified to give

$$\int_0^L \mathrm{d}x \int_0^L \mathrm{d}y\, (L - x)(L - y)\hat{\Phi}(x, y)$$
$$= -\tfrac{1}{2} \int_0^L \mathrm{d}x \int_0^L \mathrm{d}y \left(L^2 - \tfrac{2}{3}L(x + y) + \tfrac{1}{2}xy\right) \boldsymbol{r} \cdot \nabla\hat{\Phi}(x, y)$$
$$+\frac{1}{12}L^2 \int_0^L \mathrm{d}\zeta\, (2L - \zeta) \left(\hat{\Phi}(\zeta, L) + \hat{\Phi}(L, \zeta)\right). \tag{52}$$

The integration over the dummy variable implicit in the final term can be removed by a further integration by parts which yields

$$\int_0^L \mathrm{d}x \int_0^L \mathrm{d}y\, (L - x)(L - y)\hat{\Phi}(x, y)$$
$$= -\tfrac{1}{2} \int_0^L \mathrm{d}x \int_0^L \mathrm{d}y \left(L^2 - \tfrac{2}{3}L(x + y) + \tfrac{1}{2}xy\right) \boldsymbol{r} \cdot \nabla\hat{\Phi}(x, y)$$
$$+\tfrac{1}{4}L^4\hat{\Phi}(L, L) - \tfrac{1}{24}L^2 \int_0^L \mathrm{d}\zeta\, \zeta(4L - \zeta) \left\{\frac{\mathrm{d}\hat{\Phi}(\zeta, L)}{\mathrm{d}\zeta} + \frac{\mathrm{d}\hat{\Phi}(L, \zeta)}{\mathrm{d}\zeta}\right\}. \tag{53}$$

The presence of the derivative terms eliminates the integration over the dummy variable in (20), thus leaving an exact expression which requires only a double integration for evaluation.

So far attention has been confined to random fields that have square supports; this restriction can be relaxed by scaling one of the spatial variables to produce a rectangular support.

5. Comparison of theory with results of simulation

In this section, the theoretical results which have been derived are validated by comparison of their predictions with the measured properties of simulated random fields. Correlated Gaussian random fields have been generated by filtering white Gaussian noise in the frequency domain with the square root of the desired power spectrum. Two ACF shapes have been considered these being firstly a bidimensional Gaussian ACF with functional form

$$R(x, y) = \exp\left\{-a^2(x^2 + y^2)\right\} \tag{54}$$

and secondly a bidimensional, double-sided negative exponential ACF with functional form

$$R(x, y) = \exp\{-a(|x| + |y|)\}. \tag{55}$$

The images of figure 1 show random realizations of these GRFs. Figure 1(a) has been generated using the Gaussian ACF with $a = 1/\sqrt{500}$ whilst figure 1(b) has been generated using the double-sided negative exponential with $a = \frac{1}{10}$. In the former case the ACF is circularly symmetric, whilst in the latter case the ACF has stronger correlations along the grid axes. This accounts for the different textural effects in the two images.

The mean number of excursions above a threshold depends simply on the single-point statistics and is given by equation (6). The variance of the number of excursions is obtained from equations (8) and (20) and can be approximated by equation (49) for short correlation lengths. Alternative expressions for the mean and variance arise from the PDF approximation for high threshold developed by Adler [2] and are given by equation (36). Figures 2(a) and (b) show the variation of the mean and standard deviation of the percentage of above-threshold excursions for varying threshold. The full curves illustrate the simulation results, whilst the short-broken curves arise from the Adler high-threshold approximation and the long-broken curves arise from equations (6) and (49). A bidimensional Gaussian ACF was used with $a = 1$ which represents a short correlation length appropriate for the use of equation (49). It be seen that the theoretical curves derived herein provide a very good fit to the simulation

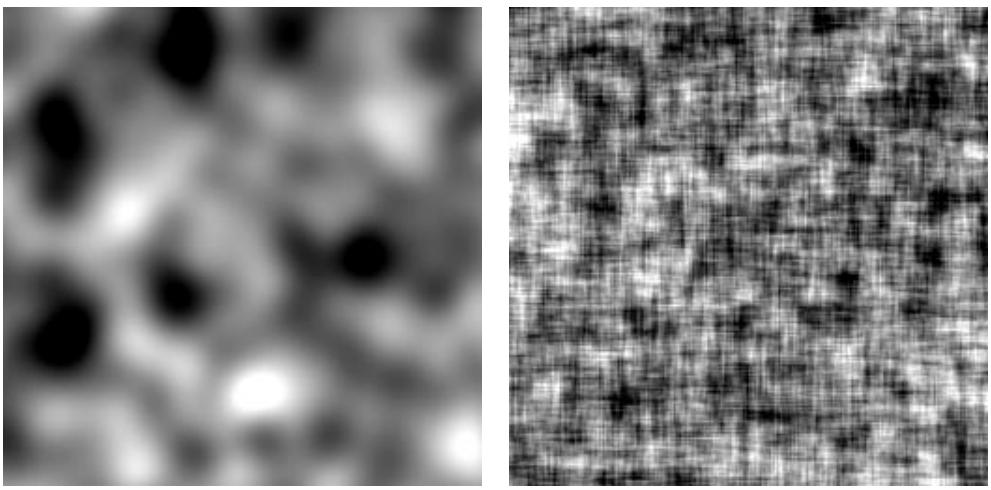

(a) (b)

Figure 1. (a) GRF realization using ACF of equation (54) and $a = 1/\sqrt{500}$; (b) GRF realization using ACF of equation (55) and $a = \frac{1}{10}$.

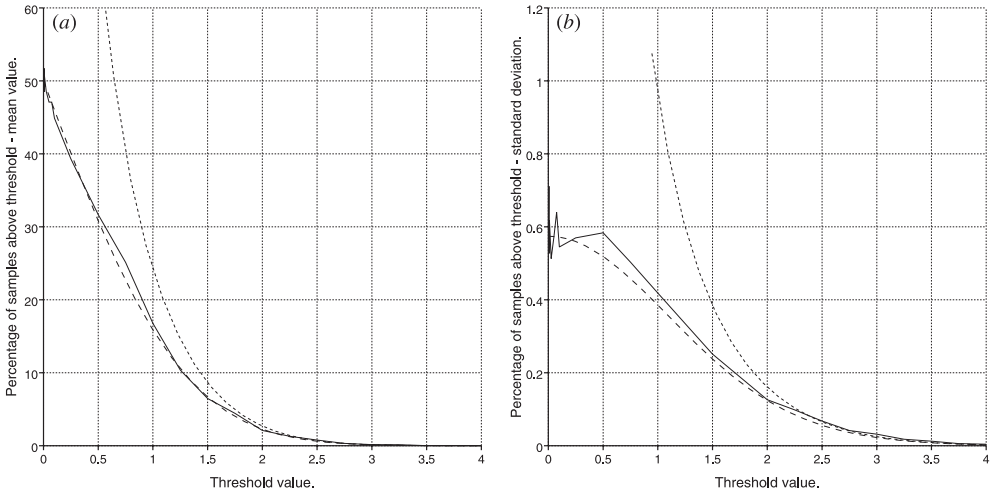

Figure 2. (*a*) Mean value; (*b*) standard deviation of the percentage of samples above threshold: full curve, simulation results; short-broken curve, Adler approximation and long-broken curve, theoretical predictions.

measurements. The Adler approximation is satisfactory at high thresholds of about three standard deviations above the mean but the predictions are very poor at lower thresholds. Thus the Adler result has been validated for the regime in which it is appropriate and indeed provides a full PDF which is appropriate in this regime. For lower thresholds, it is not valid to use the Adler approximation, but it has been shown that the first two moments can be derived theoretically, the resulting expressions having been validated against simulation results for a range of thresholds.

The standard deviation depends on the form of the ACF and in the above example a short correlation length was used so that the approximation of equation (49) was appropriate. When the correlation length becomes large in comparison with the size of the image this approximation will be less appropriate and the predictions will tend to deviate significantly from the actual behaviour. However, the exact expression of equation (53) provides an accurate prediction whatever the correlation length as is illustrated figures 3 and 4.

Each graph shows the variation of standard deviation against threshold using in figure 3(*a*) a Gaussian ACF with $a = 1/\sqrt{500}$, in figure 3(*b*) a negative exponential ACF with $a = \frac{1}{10}$, in figure 4(*a*) a Gaussian ACF with $a = 1/\sqrt{5000}$ and in figure 4(*b*) a negative exponential ACF with $a = \frac{1}{50}$. It can be seen that, as the correlation length increases, the approximation of equation (49) (short-broken curve) increasingly overestimates the standard deviation, whilst the exact expression of equation (53) (long-broken curve) provides a very good fit to the simulation results (full lines) and is thus validated.

It is interesting to note that the standard deviation for a given threshold and ACF increases as the correlation length increases. This reflects the fact that a longer correlation length allows less variation within a given image size and so there is less opportunity for statistical variations to average out within the image. There is a tendency for image values to remain within a smallish range over large areas of the image and hence to provide a correspondingly large number of threshold exceedences or non-exceedences. Thus a greater variation in the number of exceedences for a given threshold results.

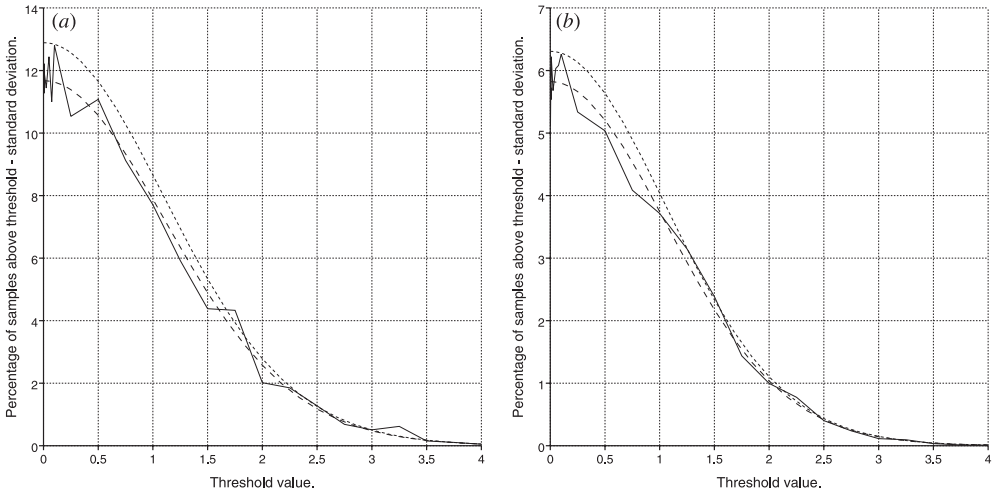

Figure 3. Standard deviation for (*a*) Gaussian and (*b*) negative exponential of intermediate correlation length using an approximation of equation (49) (short-broken curve), exact expression of equation (53) (long-broken curve) and simulation (full curves).

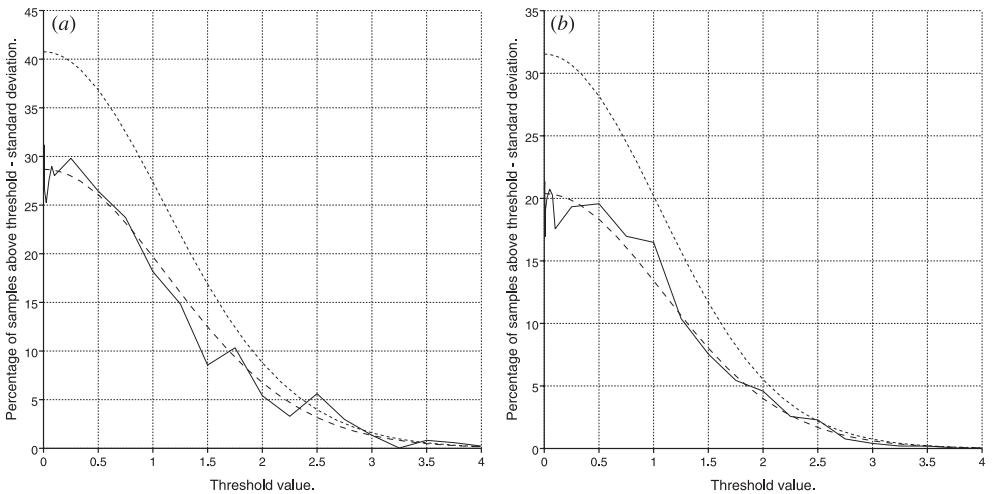

Figure 4. Standard deviation for (*a*) a Gaussian and (*b*) a negative exponential of very long correlation length using the approximation of equation (49) (short-broken curve), exact expression of equation (53) (long-broken curve) and simulation (full curves).

In section 3 it was seen how the analysis could be extended to a gamma-distributed process to produce the fundamental result of equation (44). Validation of this expression has been addressed using correlated, gamma-distributed time series together with the exact expression given by the first equality of equation (47). In this case $\phi(t)$ is given by $\hat{\sigma}(R(t))^2$ obtained from equation (44) with the first term on the right-hand side giving $\langle\sigma\rangle^2$, which is subtracted in the calculation of the variance to leave the second term on the right-hand side as the only contribution to the variance. Correlated time series were generated using the method of Armstrong and Griffiths [11] in which a number of correlated Gaussian sequences are squared and added element by element. If n sequences are used then the resulting sequence

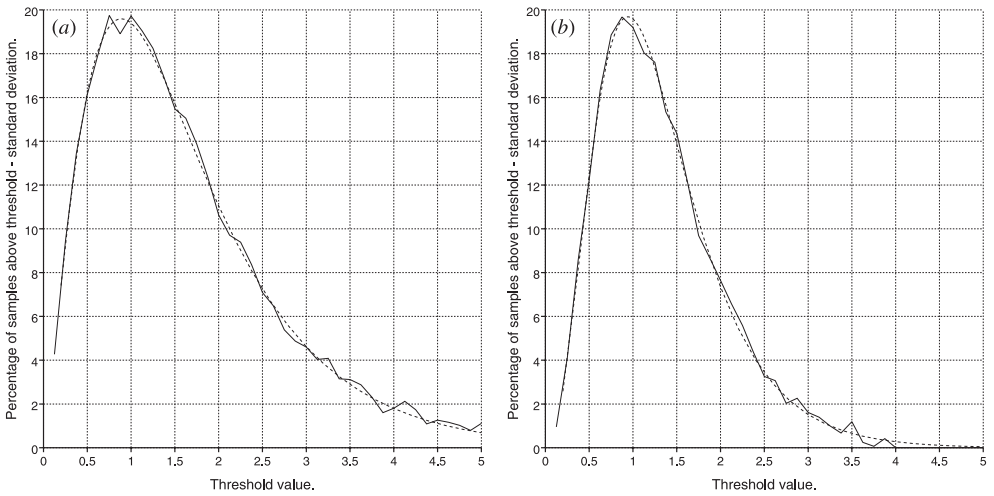

Figure 5. Standard deviation for gamma-distributed time series with unit mean and (*a*) order parameter of 2; (*b*) order parameter of 4 using exact expression of equation (47) (broken curves) and simulation (full curves).

is a correlated gamma distribution with order parameter $\nu = n/2$. Division by n after the addition was used to obtain a unit mean. The normalized ACF of the Gaussian sequences was chosen to be

$$R(t) = \exp\left(-\frac{t^2}{l^2}\right) \tag{56}$$

which must be squared to give the normalized ACF of the resulting gamma-distributed sequence. Two simulations were performed, each having $l = \sqrt{500}$, with the first using $n = 4 \Rightarrow \nu = 2$ and the second using $n = 8 \Rightarrow \nu = 4$. The variation with threshold of the standard deviation in the percentage of samples exceeding that threshold is shown in figure 5.

It can be seen that once again the exact expression gives an excellent fit to the simulated results thus validating the analysis. It should be noted that, for a given threshold, the standard deviation for $\nu = 2$ is generally greater then the standard deviation for $\nu = 4$. This is a result of the variance of the gamma distribution, $\sigma^2 = \mu^2/\nu$, being larger for smaller-order parameters and hence causing greater variation in the number of threshold exceedences.

6. Discussion and conclusions

The use of a threshold to identify anomalous statistical events is a fundamental element of statistical decision theory [13]. Of particular interest is the target detection problem in which anomalously bright pixels are identified within a statistically homogeneous region and flagged as potential targets. A false alarm occurs if a target is declared when no target is actually present as a result of statistical fluctuations of the background. It is important to know the number of times such false alarms will occur in order to understand the performance of a target detection scheme. This is given by the mean of the number of threshold exceedences and is dependent only on the single-point statistics of the background. Thus, over a large, statistically homogeneous region, there will be a single false alarm rate which is easily calculated. However, if the false alarm rate is calculated over smaller sections within this

large region it will be seen to fluctuate. Some of the smaller sections will contain very few false alarms, whilst others may contain a large number of false alarms. This will be particularly evident if the background statistical process is correlated with a correlation length which is significant in comparison to the length scale of the smaller sections. The consequent clustering of false alarms could prove deceptive if not anticipated since it could suggest a grouping of targets which might lend the hypothesis of the presence of targets more strength than would a similar number of isolated detections. For example, in a radar image of a potential battlefield, the contextual information that tanks will tend to travel in battalions may be used to reinforce an initial detection stage. A clustering of false alarms could be interpreted as such a grouping and thus the confidence that this was a true detection would be erroneously increased. Thus it is important to understand how the number of threshold exceedences per section will fluctuate from section to section so that such clustering can be anticipated. The analysis presented in this paper has derived the theoretical results which are required to assess this variation for both correlated Gaussian random fields and correlated gamma-distributed random fields. The former is relevant for detection against Gaussian noise and also for the identification of peaks in the output of a template-matching process where the central limit theorem dictates that the output of the template correlation will tend to a Gaussian distribution. The latter is relevant for detection against gamma-distributed noise which can provide a reasonable model of the non-Gaussian statistics observed in coherent imaging systems such as synthetic aperture radar or sonar.

It should be recognized that correlated random fields provide useful models for a wide variety of physical phenomena and that the results which have been presented here may well find application in fields other than image analysis and interpretation. Thus, for example, Clements and Yurtsever [8] identify above-threshold excursions of a two-dimensional Gaussian random field (representing the vertical acceleration of the ocean surface) with breaking wave events that contribute significantly to radar ocean backscatter; the statistics of the supports of these exceedences are related to those of the resulting sea clutter returns. Clements and Yurtsever evaluate the variance in sea clutter power, using a high-threshold approximation to $\hat{\sigma}(R)^2$ that is similar to but not identical to (30), incorporated into the approximate result (49). The results presented in this paper could be applied directly in this context. The use of the exact form of $\hat{\sigma}(R)^2$ would allow a more controlled test of the validity of their model. Furthermore, the corrections to (49) implicit in the exact result (53) should be of particular importance in the modelling of high resolution radar sea clutter, in which finite range cell size effects are important. Similar improvements might be anticipated in the wide range of applications of Gaussian and other random fields listed by Adler [2], about which the authors are not qualified to speculate.

Acknowledgment

This work was funded by the UK MoD Corporate Research Programme under project number 0999-3114 within Technology Group 9 (RF Technology).

References

[1] Middleton D 1960 *An Introduction to Statistical Communication Theory* (New York: McGraw-Hill)
[2] Adler R J 1981 *The Geometry of Random Fields* (New York: Wiley)
[3] Papoulis A 1965 *Probability, Random Variables and Stochastic Processes* (New York: McGraw-Hill) section 14.3

[4] Oliver C J and Quegan S 1998 *Understanding Synthetic Aperture Radar Images* (Norwood, MA: Artech House)
[5] Abramowitz M and Stegun I A 1965 *Handbook of Mathematical Functions* (New York: Dover)
[6] Kendall M G and Stuart A 1969 *Advanced Theory of Statistics* (London: Griffin)
[7] Bleistein N and Handelsman R A 1975 *Asymptotic Expansions of Integrals* (New York: Holt, Reinhart and Winston) ch 4
[8] Clements M and Yurtsever U 1997 The breaking area model for low grazing angle sea clutter Dynamics Technology Inc., 1555 Wilson Boulevard, Arlington, Virginia 22209, USA
[9] Cox D R and Miller H D 1965 *The Theory of Stochastic Processes* (London: Methuen)
[10] Blacknell D 1994 New method for the simulation of K-distributed clutter *IEE Proc., Radar Sonar Navig.* **141** 53–8
[11] Armstrong B C and Griffiths H D 1991 Modelling spatially correlated K-distributed clutter *Electron. Lett.* **27** 1355–6
[12] Wong E 1963 *Proc. Am. Math. Soc. Symp. Appl. Math.* **16** 264–76
[13] van Trees H L 1968 *Detection, Estimation and Modulation Theory* part I (New York: Wiley)